

Insulating Nickel at a Pressure of 34 TPa

A. K. McMahan

Lawrence Livermore National Laboratory, University of California, Livermore, California 94550

and

R. C. Albers

Theoretical Division, Los Alamos National Laboratory, University of California, Los Alamos, New Mexico 87545
(Received 26 July 1982)

Self-consistent augmented-plane-wave calculations are reported which predict that nickel should transform from a metal to an insulator at a pressure of 34 TPa ($\sim 340 \times 10^6$ atm), and then revert back to a metal at 51 TPa. These transitions follow from general trends in the evolution of electronic structure under compression and indicate that the richness found in the electronic structure of most solids can persist throughout, and well beyond, the pressure range of current experimental and geophysical interest.

PACS numbers: 71.30.+h, 62.50.+p, 71.25.Pi

It is widely believed that all insulators will become metals, that poor metals will become better metals, and more generally that electron energy bands in solids will simplify towards a nearly-free-electron character under the application of sufficiently high pressure. Nonetheless, there is growing theoretical evidence that this process is neither rapid nor simple. For example, solid He is not predicted to become a metal until 11 TPa,¹ while Mg is expected to undergo a metal \rightarrow semimetal \rightarrow metal transition at the still higher pressure of 24 TPa.² (One terapascal or TPa is approximately ten million atmospheres, about five times the pressure at the center of the earth.) In this paper we make an even more surprising prediction, namely, that Ni, a good metal at normal pressure (1 atm), will transform to an *insulator* at 34 TPa, before reverting back to metallic behavior at 51 TPa. These extraordinarily high pressures exceed current experimental capabilities by two orders of magnitudes,³ and pressures of geophysical interest (i.e., giant planets) by one order of magnitude. It is thus apparent that the richness found in the normal electronic structure of most solids persists throughout an enormously high range of pressure.

This metal \rightarrow insulator \rightarrow metal transition in Ni is a dramatic manifestation of two general trends which occur in the evolution of electronic structure with compression. The first trend, which is responsible for the metal-to-insulator transition in Ni, is the tendency for high-angular-momentum bands to drop in energy relative to those of lower angular momentum. This behavior reflects the different volume dependence of $V^{-2/3}$ and $V^{-1/3}$ for the one-electron kinetic and potential energies, respectively, and hence the predominance

of the kinetic energy at high compression. More specifically, if the number of radial nodes in each wave function is taken as a rough measure of the kinetic energy, then clearly the 3d states (no radial nodes) have lower kinetic energy than do the 4s states (three radial nodes), and we expect the 3d levels to rise less rapidly than the 4s levels. This expectation is clearly demonstrated in Fig. 1, where we show the unhybridized band positions for Ni as a function of compression,⁴ V_0/V , where V_0 is the zero-pressure volume of

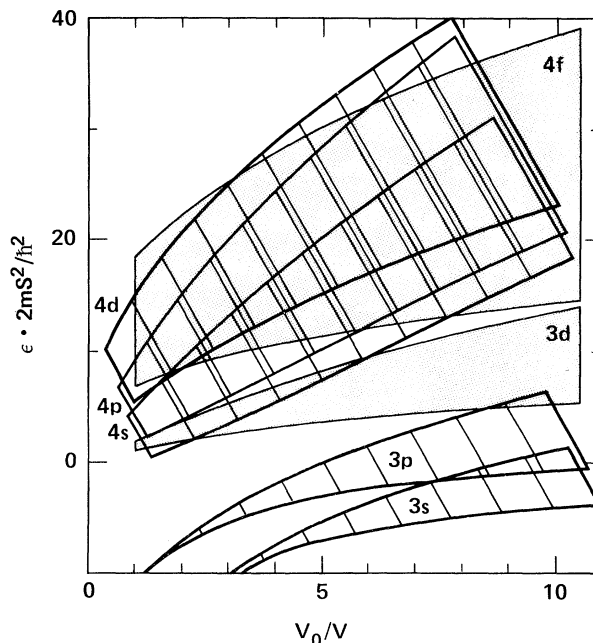


FIG. 1. Unhybridized band edges for fcc Ni as a function of compression, V_0/V . The energies, ϵ , are multiplied by $2mS^2/\hbar^2$ (V = volume per atom = $4\pi S^3/3$).

the solid.

Furthermore, since the Fermi level for Ni (on the scale of Fig. 1) is essentially right at the top of the 3*d* band, this upward motion of the 4*s* band implies a transfer of electrons from 4*s* to 3*d* levels as the solid is compressed. In fact, such *s-d* transitions are a very common phenomenon in high-pressure physics, with dramatic consequences on the measurable properties of a number of materials.⁵ In the case of Ni, the conclusion of this *s-d* transition occurs near $V_0/V=6$ (for the unhybridized calculations shown in Fig. 1), when the bottom of the 4*s* band rises completely above the 3*d* band.⁶ This leaves a full 3*d* band below a band gap, and Ni has become an insulator.

The second of the two trends is the expected band broadening with compression as orbitals on adjacent atoms begin to overlap more strongly. It is primarily this behavior which is responsible for returning Ni to metallic character when the continued broadening of both the 3*d* and 4*f* bands causes them to eventually overlap and hence close the insulating gap.

The main calculations reported in the present paper have been carried out for zero-temperature fcc Ni using the self-consistent, nonrelativistic, augmented-plane-wave (APW) technique,⁷ except where indicated otherwise. Exchange and correlation were treated by the von Barth-Hedin potential.⁸ Although the calculations were not spin polarized, the behavior of Fe suggests⁹ that the non-spin-polarized solution should become the energetically favored solution at high compression,

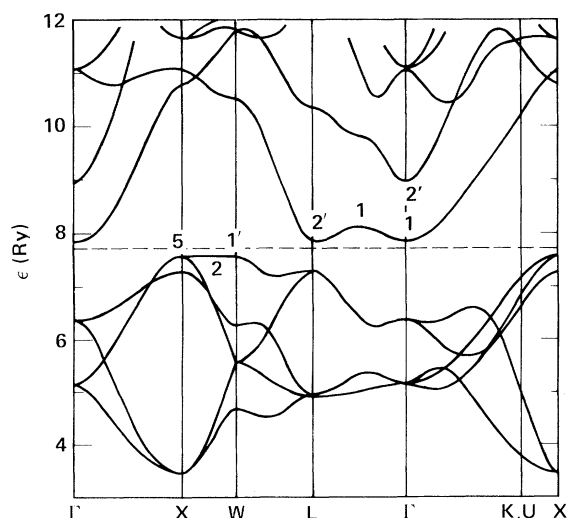


FIG. 2. Nonrelativistic APW band structure of fcc Ni at $V_0/V=7.5$. The dashed line is the Fermi level.

sions, and long before the range of interest in this work. All electrons were treated self-consistently with the uppermost 18 electrons (i.e., including 3*s* and 3*p*) treated in a band mode for compressions $V_0/V \geq 2$, and the uppermost 16 for $V_0/V < 2$. The Brillouin zone was sampled with sufficient points (256 or 2048 in the full zone) to insure convergence of both the pressure and relevant energy gaps to within a few percent. Interpolation of three low-pressure points near $V_0/V \sim 1$ gives a zero-pressure lattice constant of 6.54 bohrs, in excellent agreement with other non-spin-polarized calculations for Ni.¹⁰

Figure 2 shows the APW band structure⁴ for fcc Ni at $V_0/V=7.5$. The Fermi level (dashed line) is placed midway in the insulating gap, above the full 3*d* band. The $W_{1'}$ level is the highest-energy 3*d* state for the range of compressions of interest here, although the $X_5-Z_2-W_{1'}$ branch is very nearly degenerate in energy. The Γ_1 (4*s*) and $L_{2'}$ (4*f*) are the lowest levels above the gap, and are approximately degenerate in energy at this compression. Test calculations using 16 384

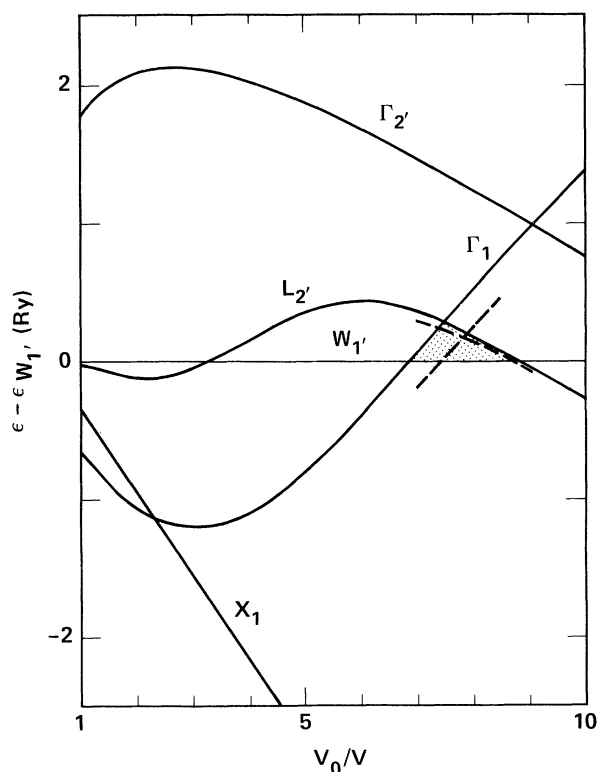


FIG. 3. One-electron energies for fcc Ni as a function of compression, V_0/V . The nonrelativistic results are the solid lines; the scalar-relativistic, the dashed lines. The shaded region shows the insulating gap.

points in the full Brillouin zone showed that these W , Γ , and L levels do indeed delimit the gap.

The dependence of the insulating gap on compression for these fully hybridized calculations is shown in Fig. 3, where the high symmetry eigenvalues are plotted relative to the W_1' level. At $V_0/V = 7$ the bottom of the $4s$ band (Γ_1) rises above the top of the $3d$ band (W_1') creating the insulating gap, which is shaded. The L_2' level is of mixed $4p$ and $4f$ character and initially rises (for $V_0/V > 2$) in response to the upward motion of the $4p$ band, but then bends downward as it becomes more $4f$ -like. This may be judged by comparison to the motion of the Γ_2' level which is of pure $4f$ character. In these nonrelativistic calculations the gap is largest at $V_0/V = 7.5$ where the Γ_1 and L_2' levels cross. At this point the gap is 0.27 Ry (3.7 eV), which is 6% of the $3d$ bandwidth (the X_1 to W_1' separation). Table I lists the various gap energies, as well as the calculated pressures, as a function of V_0/V .

The existence of the insulating gap in highly compressed Ni is the essential point of this paper. Since the gap is relatively small in comparison to the $3d$ bandwidth, we have taken some pains to ascertain its sensitivity to the approximations inherent in our calculations. These tests, which we discuss in the remainder of the paper, confirm the existence of the gap. In addition, we have found that the gap also exists for the less-stable¹¹ hcp and bcc structures in the volume region where the fcc gap is largest.

Self-consistent, nonrelativistic, linear-muffin-tin-orbital (LMTO) calculations^{12,13} yield the

TABLE I. Nonrelativistic APW results for $T = 0$ fcc Ni as a function of compression, V_0/V . The zero-pressure volume, V_0 , corresponds to the observed $T = 298$ K lattice constant, $a = 6.660$ bohrs. Pressures, P , are in terapascals, and the one-electron energy separations, ϵ , are in rydbergs.

V_0/V	P	$\epsilon(\Gamma_1 - W_1')$	$\epsilon(L_2' - W_1')$
1	-0.0109	-0.642	-0.022
1.1	0.0107	-0.693	-0.038
1.2	0.0429	-0.743	-0.054
2	0.666	-1.045	-0.109
4	6.22	-1.088	0.171
6	18.7	-0.409	0.413
7	28.2	0.045	0.341
7.5	33.9	0.282	0.270
8	40.2	0.515	0.182
10	71.8	1.364	-0.267

same qualitative results as seen in Fig. 3, but with an insulating gap at $V_0/V = 7.5$ about twice the size of that obtained from the APW method. After achieving self-consistency, the gap was computed by linearizing in the gap region, retaining angular momentum components through h character, and including the combined-correction term to the atomic sphere approximation (ASA) used in the LMTO method.¹² Omitting this correction term further increased the $L_2' - W_1'$ separation by a factor of 2.4, pointing to the ASA approximation as the likely cause of the difference between the LMTO and APW results. Although both APW and LMTO methods are in qualitative and generally good quantitative agreement, we have reported the APW calculations in more detail because they give a more conservative (i.e., smaller) insulating gap, and should also be somewhat more rigorous.

Since our APW program cannot be run in a relativistic mode, we have evaluated the mass velocity and Darwin shifts in the one-electron energies by comparing nonrelativistic and scalar-relativistic (by scalar we mean neglecting spin orbit) self-consistent LMTO calculations. When the resulting relativistic shifts in the $\Gamma_1 - W_1'$ and $L_2' - W_1'$ separations are added to the nonrelativistic APW results in Fig. 3, the insulating gap is reduced to the portion of the shaded area lying below the two dashed lines. The maximum gap now occurs at $V_0/V = 7.9$ and is 0.17 Ry (2.3 eV) in size. As a further check, eigenvalues were recalculated at $V_0/V = 7.5$ by a scalar-relativistic linearized-APW program¹⁴ using a self-consistent, scalar-relativistic LMTO potential.¹⁵ The $\Gamma_1 - W_1'$ separation was found to be essentially identical to that shown by the dashed lines in Fig. 3, while the $L_2' - W_1'$ separation was smaller by only 19%.

Spin-orbit coupling parameters,¹⁶ ξ_l , were calculated at $V_0/V = 7.5$ by using the scalar-relativistic LMTO wave functions, and were found to be negligible ($\xi \leq 0.013$ Ry) with the exception of $\xi_p = 0.17$ Ry. Accordingly there can be no significant shift of the $X_5 - Z_2 - W_1'$ branch ($l \geq d$), splitting of X_5 , nor shift of the pure s Γ_1 level. The L_2' level is about 20% p character at $V_0/V = 7.9$, and so at worst a spin-orbit shift of this level could only reduce the scalar-relativistic gap by 20%.

It is well known that local density calculations generally underestimate insulating gaps near ambient conditions, especially when potentials such as that of von Barth and Hedin⁸ are used. This is believed to be due to the inadequate treat-

ment of correlation which causes differing relative errors for states bounding the gap because of their different degrees of localization. Given the huge compressions of interest here, and the highly nonlocalized nature of all states, this is not likely to be a problem. Indeed, we find that self-consistent APW calculations using the Kohn-Sham exchange potential,¹⁷ i.e., omitting any approximation to correlation whatsoever, yields the same gap (within 5%) at $V_0/V = 7.5$ as that obtained with the von Barth-Hedin potential.

In summary, we suggest that Ni will exist in an insulating state near $V_0/V = 7.9$ for temperatures $T < 0.017$ Ry (to preclude thermal excitation, T is limited to less than a tenth of the gap¹⁸). This regime is accessed by isentropic compression from $V_0/V = 1$ and $T < 200$ K, requiring an energy of about 13 Ry/atom to achieve the compression.

This work was performed under the auspices of the U. S. Department of Energy by Lawrence Livermore and Los Alamos National Laboratories under Contracts No. W-7405-Eng-48 and No. W-7405-Eng-36.

¹D. A. Young, A. K. McMahan, and M. Ross, Phys. Rev. B **24**, 5119 (1981).

²J. A. Moriarty and A. K. McMahan, Phys. Rev. Lett. **48**, 809 (1982).

³We exclude shock compression techniques [e.g., C. E. Ragan, III, Phys. Rev. A **21**, 458 (1980)], which can achieve 10 TPa pressures, but which heat the sample to very hot, dense plasma conditions.

⁴All of our results are from fully hybridized calculations, except Fig. 1, where we computed the band-edge positions from APW potentials by using a method similar to the Wigner-Seitz rules. The energy zero in Figs.

1 and 2 is the muffin-tin zero.

⁵See, e.g., M. Ross and A. K. McMahan, Phys. Rev. B **26**, 4088 (1982), and references therein.

⁶Copper has the same behavior in this pressure range, R. C. Albers, A. K. McMahan, and J. E. Müller, to be published.

⁷For a detailed description, see M. Ross and K. W. Johnson, Phys. Rev. B **2**, 4709 (1970); A. K. McMahan and M. Ross, Phys. Rev. B **15**, 718 (1977).

⁸U. von Barth and L. Hedin, J. Phys. C **5**, 1629 (1972).

⁹O. K. Andersen, J. Madsen, U. K. Poulsen, O. Jepsen, and J. Kollar, Physica (Utrecht) **86-88B**, 249 (1977).

¹⁰V. L. Moruzzi, J. F. Janak, and A. R. Williams, *Calculated Electronic Properties of Metals* (Pergamon, New York, 1978).

¹¹The scalar-relativistic, linear-muffin-tin-orbital, force-relation technique described in Ref. 2 was used to determine phase stability. For the hcp structure, we find an insulating gap throughout the range of c/a investigated, from 1.4 to 1.85. The most stable hcp phase was found near the ideal c/a ratio, 1.633.

¹²O. K. Andersen, Phys. Rev. B **12**, 3060 (1975); O. K. Andersen, Europhys. News **12**, 4 (1981).

¹³The LMTO program used was a modification of a program kindly provided by Dr. H. L. Skriver, and is described in A. K. McMahan, H. L. Skriver, and B. Johansson, Phys. Rev. B **23**, 5016 (1981).

¹⁴J. E. Müller, thesis, Cornell University, 1980 (unpublished); J. E. Müller and J. W. Wilkins, to be published.

¹⁵A version of the LMTO program described in Ref. 13 was used which generates a muffin-tin potential.

¹⁶F. Herman and S. Skillman, *Atomic Structure Calculations* (Prentice-Hall, Englewood Cliffs, N. J., 1963).

¹⁷W. Kohn and L. J. Sham, Phys. Rev. **140**, A1193 (1965).

¹⁸Self-consistent, finite-temperature LMTO calculations at $V_0/V = 7.5$ show only a slight temperature dependence of the gap in this region, although a 35% increase by a temperature equal to twice the $T = 0$ gap.